

Marcelina Kasińska, Tomasz Piwowarczyk, Wiesław Derlukiewicz, Piotr Fijołek

Assessment of Macro and Microstructure of Welded Joints Made of Steel P265GH Using Various Combinations of Welding Consumables

Abstract: The article presents the assessment of the macro and microstructure of welded joints made in steel P265GH using various combinations of filler metal wires and shielding gases. In addition to microstructural analysis, tests involved hardness measurements of all of the joint zones, i.e. the weld, HAZ and the base material. In addition, each specimen (i.e. the weld and the base material) was subjected to the analysis of chemical composition. The performed analysis made it possible to determine the degree of morphological conformity of welding consumables with steel P265GH.

Keywords: welded joints, steel P265GH, welding consumables,

DOI: [10.17729/ebis.2018.4/3](https://doi.org/10.17729/ebis.2018.4/3)

Introduction

The Polish power generation sector is based on system power plants (19 heat and power plants and 5 water-power plants) [1]. The professional power engineering is supported by scattered power engineering (heat and power plants and water-power plants) [2,3]. Present investments include 5 power units (commissioning expected by 2019) [3,4]. At the same time it should be emphasized that nearly 90% of currently operated power units have exceeded their nominal work time of 100 000 h. In addition, a significant number of such units has also exceeded a work time of 200 000 hours (the units were approved for 300 000 hours of operation) [1-4].

Because of the complexity of factors limiting the operational usability of power generating systems as well as the extent of the operational

time-span of objects and systems approved for further operation, the issue of utmost importance is the diagnostics of elements and entire units as well as the determination of their operational and terminal service life [1,4]. The diagnostics of such objects and elements primarily includes non-destructive tests, mostly penetrant tests (PT), magnetic-particle tests (MT), ultrasonic tests (UT), visual/endoscopic tests (VT) as well as structural tests including the method of matrix and extraction replicas and the X-ray phase analysis of carbide isolates [1,4-9]. Other activities include material-related assessments of elements in view of their further operation as well as safe and failure-free operability and the qualification of elements including the planning of inspections, repairs, revamping, modernisation or liquidation [1,10-14].

inż. Marcelina Kasińska (Eng.); dr inż. Tomasz Piwowarczyk (PhD (DSc) Eng.); dr inż. Wiesław Derlukiewicz (PhD (DSc) Eng.) – Wrocław University of Technology, Faculty of Mechanical Engineering, Division of Materials Science; inż. Piotr Fijołek (Eng.) – PB TEST – Technical Tests and Measurements, Wrocław

The primary issue related to the service life of elements exposed to high-temperature operation is the creep phenomenon. Factors significantly limiting the service life of power generating objects are also welded joints, or more precisely their durability and reparability (by making repair joints). This issue is of particular importance in cases of the so-called dissimilar (“mixed”) joints, where the welding-based repair process involves an old material (in operation) with a new one. Another important issue is the implementation of structural changes, among other things, during revamping or repairs [1,4]. When forecasting the service life of units exposed to creep conditions it is important to know not only characteristics concerning creep-related properties but also characteristics related to changes in the structures of materials affected by stresses in the function of time and temperature at the same time [1,4].

Taking into consideration the present state of the power engineering sector (operation of equipment exceeding the nominal work time) and forecasts predicting very few investments, the Office of Technical Inspection (Urząd Dozoru Technicznego – UDT) has imposed new obligations (in the form of guidelines) on the owners of power plants/heat and power stations as well as on the external technical inspection services [1,4,15-16]. This document explicitly indicates the obligation of preceding each repair involving joining processes by microstructural tests and other tests involving NDT methods (previously, this issue was usually ignored). Only after the obtainment of the positive result of the above-named tests it is possible to perform repairs taking into consideration specialist joining instructions and the schedule of tests and inspections [15-16]. In addition to changes in regulations concerning the construction, revamping and operation of elements of power generating objects, ongoing works are also concerned with the development of new generation materials applicable in the power generation

sector. Factors significantly affecting the nature of these tests are undoubtedly restrictions related to environmental conditions and constantly rising coal prices. The use of materials characterised by more favourable properties makes it possible to increase the efficiency of power generating equipment through the more effective combustion of fuels, and, consequently to reduce harmful emissions into the atmosphere and decrease the consumption of fuel [1,4].

The issues related to the analysis of the properties of welded joints made of steel P265GH was presented in publication [1], constituting the introduction to this publication. Following the guidelines of the PN-EN ISO 15614-1 standard, the tests involved the making and analysing butt joints and T-joints using various combinations of filler metal wires and shielding atmospheres. The tests discussed in this study extend the entire research by including the analysis of the chemical composition, linear hardness measurements as well as the assessment of macro and microstructures of the base material, HAZ and filler metal.

Test specimens

The tests were performed using specimens sampled from test plates subjected to MAG welding (135) performed in accordance with the guidelines specified in PN-EN 15614-1, using related welding parameters. The base material was steel P265GH, commonly used in the power engineering industry, particularly in areas, where elements made of conventional structural steels could age and wear very quickly. Components made of the above-named steel (P265GH) are characterised not only by resistance to high temperature and a heating medium as well as substances contained in corrosive media [1,4]. As a result, steel P265GH is applied in the nuclear power engineering, among other things, as a material used in the nuclear power containment.

Application conditions specified by the Office of Technical Inspection (UDT) [15] do not

contain guidelines imposing the necessity of analysing microstructures of steel P265GH. Among other things, the guidelines are concerned with certain low-alloy and high-chromium steels. However, taking into consideration the popularity of the steel, the above-named application areas, the potential of making dissimilar joints and the availability of filler metal wires of various chemical compositions (dedicated according to the manufacturers of steel P265GH), the performance of in-depth analysis aimed to elevate the engineering awareness of potential users seems more than justified.

The MAG welding parameters were adjusted on the basis of initial tests. The research involved joints made of 8 mm thick plates: butt joints (BW – butt welds) (scarfing of 60°, a threshold of 2 mm and a gap of 3 mm) and T-joints (FW – fillet welds). The tests were performed using gas mixtures and filler metals presented in Table 1. Table 2 presents the chemical compositions of the shielding gases and filler metals. All of the filler metals and shielding gases were selected on the basis of guidelines specified in PN-EN ISO 14175 and PN-EN ISO 14341/ER70S-6 according to AWS A5.18. Initially, the plates were subjected to non-destructive tests, i.e. visual tests (VT 100%) and magnetic-particle tests (MT 100%) followed by destructive tests, i.e. tensile tests, bend tests and impact strength tests [1].

Table 1. Filler metals and techniques used when making the specimens

Spec. no.	Filler metal	Gas	Runs
BW1	SG2 magmate φ=1 mm	M21	3
FW1			1
BW2	SG2 magmate φ =1 mm	M25	3
FW2			1
BW3	SG2 bronze φ =1.2 mm	M21	3
FW3			1
BW4	SG2 bronze φ =1.2 mm	M25	3
FW4			1

Analysis of the chemical composition

The analysis of the chemical composition was performed using the spectral method and a GD-5500A analyser (LECO). The results of the chemical composition analysis concerning the butt joints in the weld area and the base material are presented in Table 3. The table also presents the maximum values of the chemical elements (for heat analysis) according to PN-EN 10028-2. The base material was designated as BM, whereas weld areas of specific specimens were designated as S1-S4.

The analysis of the chemical composition of the base material did not reveal any significant deviations from information concerning the contents of chemical elements specified by the PN-EN 10028 standard. The analysis of the chemical composition of the welded joints in the weld area (specimens S1-S4) did not reveal

Table 2. Chemical composition and designations of shielding atmospheres and filler metal wires [based on the data provided by the producers]

Chemical composition of shielding atmospheres

Commercial name	PN-EN ISO 14175	Chemical composition, %
CORGON 18	M21	82%Ar+18%CO ₂
CORGON 2	M25	83%Ar+13%CO ₂ +4%O ₂

Chemical composition of filler metal wires

Wire	C	Mn	S	P	Si	Cu	Ni	Cr	Al	Mo	Ti	V	N
SG2 magmate	0.08	1.50	0.013	0.011	0.880	0.029	0.020	0.021	-	-	-	-	-
SG2 bronze	0.07	1.45	0.005	0.009	0.875	0.035	0.002	0.046	0.002	0.013	0.001	0.002	0.006

Table 3. Chemical composition of the base material and butt-welded joints

	C, %	Mn, %	Si, %	P, %	S, %	Cr, %	Ni, %	Mo, %	V, %	Cu, %
BM	0.164	0.972	0.278	0.018	0.007	0.04	0.022	0.001	0.002	0.025
BM*	≤0.2	0.8-1.4	≤0.4	0.025	0.015	≤0.3	≤0.3	≤0.08	≤0.02	≤0.3
S1	0.104	1.29	0.731	0.024	0.013	0.027	0.02	-	-	0.09
S2	0.136	1.23	0.691	0.016	0.008	0.041	0.019	0.002	-	0.043
S3	0.106	1.26	0.744	0.016	0.008	0.041	0.012	0.002	-	0.081
S4	0.096	1.26	0.727	0.024	0.014	0.016	0.023	-	-	0.096

BM – base material; values obtained experimentally in the chemical composition analysis

BM* - base material, max. contents of chemical elements according to PN-EN 10028-2

S1-S4 – weld, values obtained experimentally in the chemical composition analysis

significant differences. In relation to all of the specimens, the content of carbon amounted to approximately 0.1% (or 0.136% in relation to specimen s2). The above-named values were lower than those concerning the base material. The values of the primary alloying elements, i.e. Mn and Si, were very similar (~1.25% Mn and ~0.7% Si). As regards impurities in the weld, both phosphorus and sulphur adopted values acceptable by the standard related to steel P265GH.

Differences in the content of nickel reflected the degree of its presence in the base material and in the filler metal wire. The addition of molybdenum in wire SG2 bronze left a trace in specimens s2 and s3. Copper passed to the weld area. In relation to all combinations of the filler metals the content of Cu was nearly 3-times higher than in the base material and in the filler metal. The results of the chemical composition analysis performed in relation to the test steel were used to calculate the carbon equivalent (CEV = 0.34%). The above-presented value indicated high weldability (yet inly in relation to cold cracking; the value of Mn was relatively low, which could lead to hot cracking).

Macroscopic observations

Macroscopic observations involved metallographic specimens of the butt joints containing the butt welds (BW) made in the flat position (Fig. 1) and the T-joints containing the fillet welds (FW) made in the horizontal position (Fig. 2).

All of the joints were characterised by the uniform face of the butt weld and the uniform root. Each metallographic specimen was characterised by a delicately outlined HAZ. All of the joints contained welding imperfections, i.e. excess weld metal (502). The welding imperfections were classified as representing quality level C according to PN-EN ISO 5817. The tests were also based on the guidelines of the PN-EN ISO 15614-1 standard. In accordance with the above-named document, a welding technology is qualified if the detected imperfections do not exceed upper limits specified for quality level B according to PN-EN ISO 5817. Welding imperfections related to quality level C include excess weld metal (502), excessive convexity of the fillet weld (503), excessive thickness of the fillet weld (5214) and excessive penetration (504). All of the joints revealed the banded structure of the base material having the form of a darker band located at the half of the base material thickness (particularly visible on the right side of specimen BW2). The revealed structure did not affect the quality or strength of the welded joint. The structure was composed of pearlite (resulting from the rolling of plates), undergoing etching faster than the remaining areas of the microstructure.

All of the T-joint specimens (Fig. 2) were also characterised by the uniform face of the fillet weld. The HAZ was delicately outlined in all of the cases. The narrowest HAZ was observed in relation to FW3 (Fig. 2c). Except for FW4 on the right side, slightly penetrating the

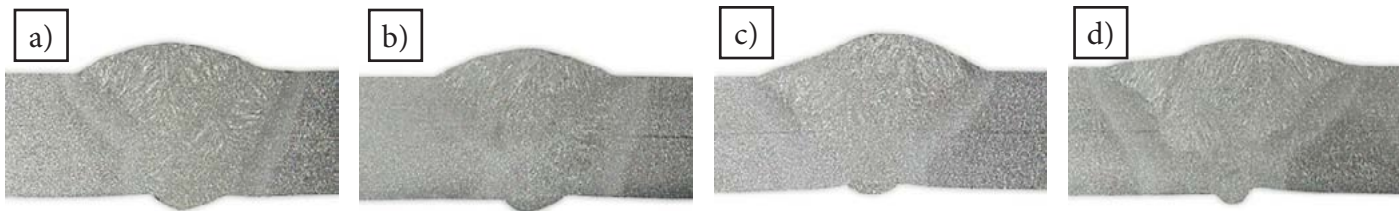


Fig. 1. Macrostructures of the butt joints: BW1 (a), BW2 (b), BW3 (c) and BW4 (d)

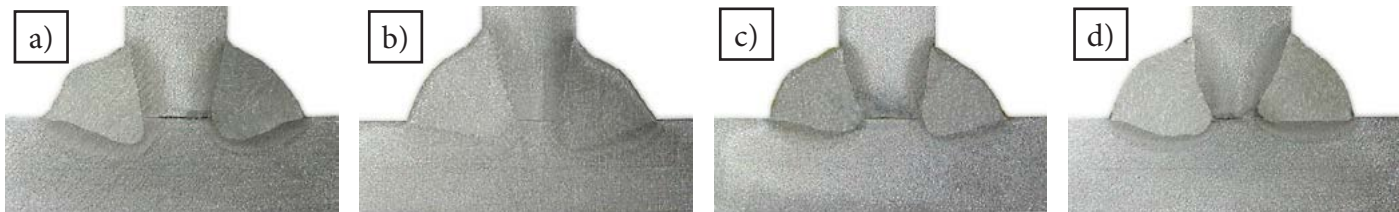


Fig. 2. Macrostructures of the T-joints: FW1 (a), FW2 (b), FW3 (c) and FW4 (d)

base material, all of the joints revealed proper penetration. All of the specimen were characterised by the slight asymmetry of the fillet weld (welding imperfection no. 512). It was also possible to notice (locally) the excessive convexity of the fillet weld face (imperfection no. 503 – e.g. the left side of FW1), yet the ascertained dimensions were not critical. Specimen FW2 (Fig. 2b) revealed an imperfection in the form of an improper gap in the root of the fillet weld (617). None of the specimens contained porosity, cracks or gas cavities.

Microscopic observations

Microstructural observations were performed at a magnification of 100x and 500x. The observations were concerned with the weld, the fusion line and the HAZ. Figure 3 presents the base material microstructure adopted as the base microstructure. The observations revealed the banded ferritic-pearlitic structure with cementite in pearlite of the lamellar and irregular structure.

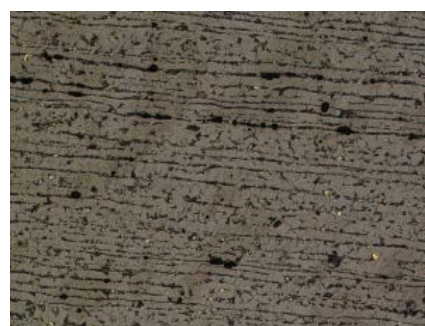


Fig. 3. Microstructure of base material P265GH – magnification 100x

Figure 4 presents the microstructure of the weld area of the welded joints. Specimen BW1 contained acicular ferrite with the features of Widmannstätten structure and slight microstructural discontinuities (Fig. 4a). Specimen BW2 contained fine grains of ferrite with visible microstructural discontinuities (Fig. 4b). Specimen BW3 contained the fine-grained irregularly arranged ferritic structure, without the features of the Widmannstätten structure, yet with slight microstructural discontinuities (Fig. 4c). Specimen BW4 contained the fine-grained ferritic structure with numerous microstructural discontinuities (Fig. 4d).

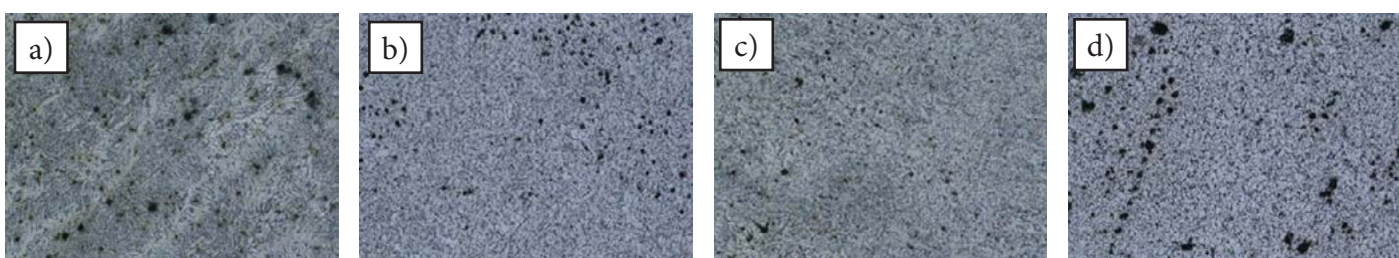


Fig. 4. Macrostructures of the welds areas in the butt joints: BW1 (a), BW2 (b), BW3 (c) and BW4 (d)

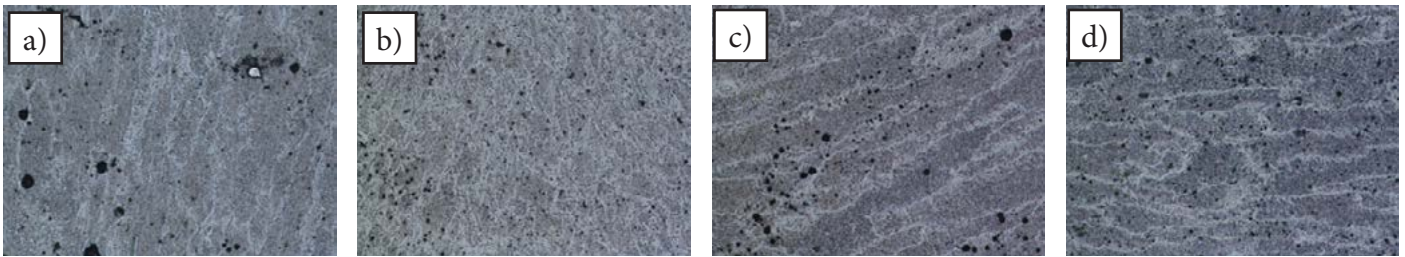


Fig. 5. Macrostructures of the welds areas in the T-joints: FW1 (a), FW2 (b), FW3 (c) and FW4 (d)

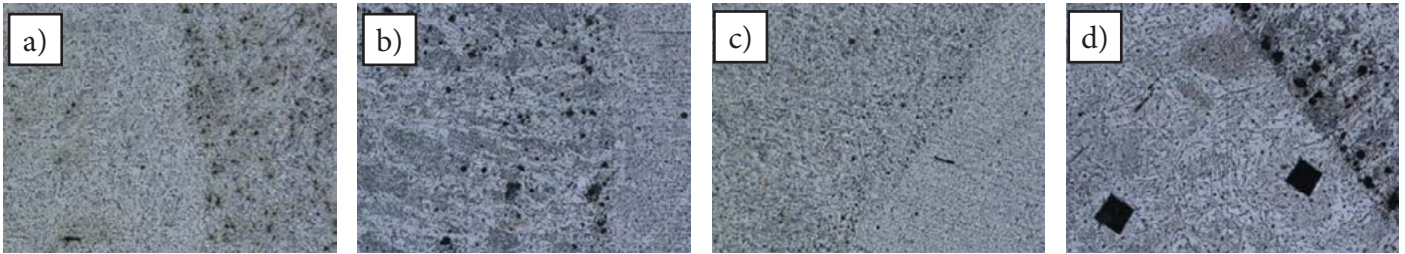


Fig. 6. Macrostructures in the fusion line of the butt joints: BW1 (a), BW2 (b), BW3 (c) and BW4 (d)

All of the T-joint specimens (FW1-FW2) were characterised by the presence of granular and acicular ferrite with areas of quasi-eutectoid (Fig. 5). The specimens also contained microstructural discontinuities.

Figures 6 and 7 present microstructures present in the fusion line of the butt and T-shaped specimens. In terms of the butt welds, the HAZ of specimen BW1 (on the base material side) was characterised by the non-equilibrium ferritic structure containing traces of pearlite (Fig. 6a). It was also possible to notice chain-like arranged fine carbides. The fusion line and the base material contained slight microstructural discontinuities (microporosity). The weld material contained ferrite with slight elements of Widmannstätten structure. The HAZ of specimen BW2 revealed the banded structure (Fig. 6b). The fusion line did not reveal the presence of welding imperfections. The weld material was characterised by the significant amount of ferrite having the bainitic structure and irregular ferrite grains. The specimen also contained

irregularly scattered microstructural discontinuities. The material of the weld and that of the HAZ in specimen BW3 did not reveal the presence of visible welding imperfections (Fig. 6c). The HAZ was characterised by the banded structure containing ferrite with a slight amount of pearlite. The fusion line contained single structural discontinuities. The fusion line and the HAZ of specimen BW4 contained numerous chain-like arranged and scattered structural discontinuities (Fig. 6d). The HAZ contained acicular ferrite with slight areas of irregular pearlite. The weld material contained ferrite having the bainitic structure.

In terms of the fillet welds (FW1-FW4), the HAZ of all of the specimens was characterised by the acicular martensitic-bainitic structure containing irregularly arranged grains of ferrite (Fig. 7).

Figures 8 and 9 present the HAZ areas of the test specimens. In terms of specimen BW1, the butt joints contained acicular ferrite with the features of Widmannstätten structure and slight

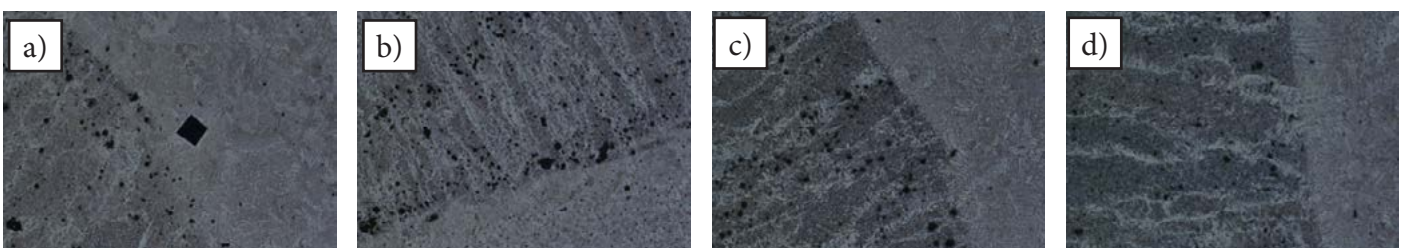


Fig. 7. Macrostructures in the fusion line of the T-joints: FW1 (a), FW2 (b), FW3 (c) and FW4 (d)

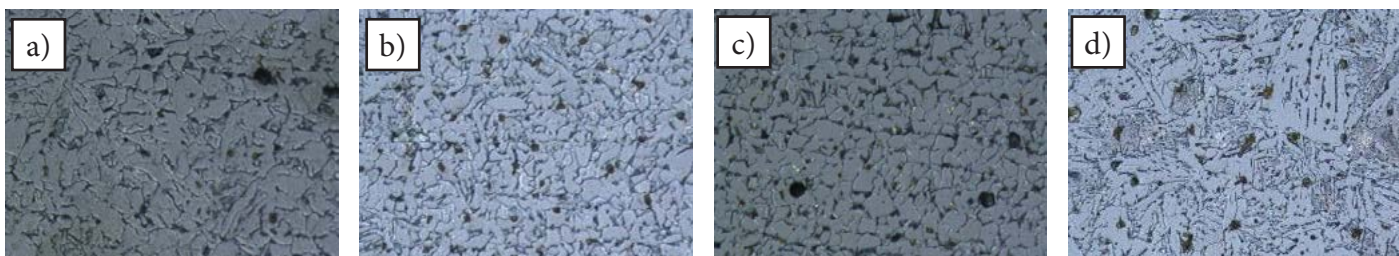


Fig. 8. Macrostructures in the HAZ area of the butt joints: BW1 (a), BW2 (b), BW3 (c) and BW4 (d)

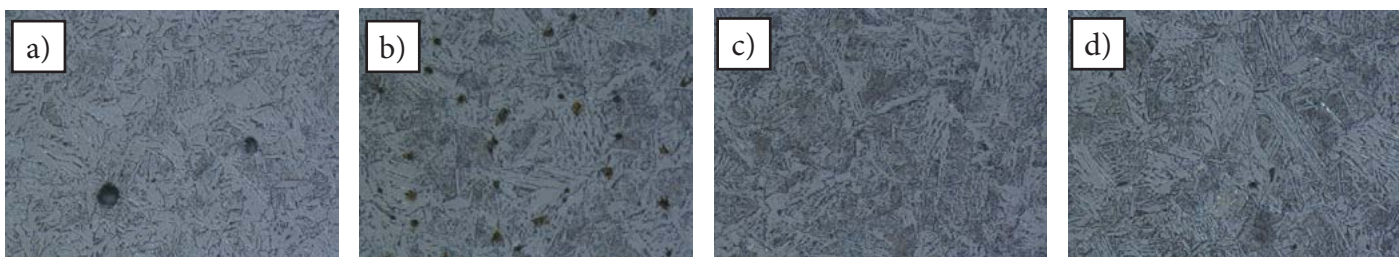


Fig. 9. Macrostructures in the HAZ of the T-joints: FW1 (a), FW2 (b), FW3 (c) and FW4 (d)

microstructural discontinuities (Fig. 8a). Specimen BW2 contained non-equilibrium grains of ferrite (Fig. 8b). Specimen BW3 contained regular ferritic grains and single areas of pearlite (Fig. 8c) as well as few microstructural discontinuities and copper visible on grain boundaries. Specimen BW4 revealed the irregular ferritic structure with the features of Widmannstätten structure (Fig. 8d). All of the T-joints were characterised by the structure of acicular ferrite with some martensitic areas (Fig. 9). Only specimen FW1 was characterised by non-equilibrium ferrite of variously sized grains (Fig. 9a) and some microstructural discontinuities.

The weld areas in all of the test specimens contained the ferritic structure. The T-joints contained granular and acicular ferrite with noticeable areas of quasi-eutectoid. The microstructural analysis of the HAZ of the welded joints revealed the presence of the ferritic structure containing variously sized grains with

a slight amount of pearlite (grain boundaries contained, locally, alloying elements).

Hardness measurements

Linear hardness measurements were performed using the Vickers test and a load of HV10. Steel P265GH belongs to material group 1.1 (according to ISO/TR 15608) having yield point $R_{e} \leq 275$ MPa. The above-named material does not reveal sensitivity to the presence of hardenings in the HAZ. The maximum allowed hardness of the above-named material amounts to 380 HV10 without heat treatment and 320 HV10 with heat treatment [2]. The hardness measurements did not reveal significant differences concerning the specimen-related hardness ranges in the function of the welding materials. In all of the specimens, regardless of the filler metal wire-shielding gas combination, the hardness measured in the weld area was significantly lower than the values permissible for P265GH

Table 4. Averaged hardness values of the but joints with the marked areas subjected to the measurements (BM – base material, HAZ – heat affected zone, W- weld)

Specimen no.	BM	HAZ	W	HAZ	BM
BW1	156	150	166	157	150
BW2	145	150	170	153	144
BW3	157	173	174	153	144
BW4	149	148	162	144	143

Table 5. Averaged hardness values of the T-joints with the marked areas subjected to the measurements (BM – base material, HAZ – heat affected zone, W- weld)

Specimen no.	BM	HAZ	W	HAZ	BM
FW1	160	181	232	190	162
FW2	161	195	225	184	171
FW3	157	179	220	189	180
FW4	167	188	224	173	167

(max do 250 HV₁₀). Table 4 presents the averaged values of the hardness measurements concerning the butt joints (with the marked areas subjected to the measurements). Table 5 presents the averaged values of the hardness measurements concerning the T-joints (with the marked areas subjected to the measurements).

Summary

The specimens used in the tests were sampled from the test plates subjected to welding in accordance with instructions specified in the PN-EN ISO 15614-1 standard. Neither destructive nor non-destructive tests revealed the presence of welding imperfections referred to in standards harmonised with PN-EN ISO 15614-1. The entire results of the tests are presented in publication [1].

The analysis of the chemical composition revealed the conformity of the chemical composition of the material subjected to the test with the guidelines specified in the PN-EN 10028-2 standard. The foregoing was used to analytically identify the value of carbon equivalent ($CEV=0.34\%$). The welds obtained in the tests were characterised by the chemical composition similar to that of the base material. In relation to the guidelines of the PN-EN 10028-2 standard, only the amount of silicon exceeded the maximum ultimate values. The above-named silicon excess was caused by its increased content in the filler metal wire.

The analysis of hardness distributions did not reveal the presence of areas characterised by increased or decreased hardness as regards related requirements. None of the measurement points revealed a value in excess of 380 HV (maximum ultimate limit in relation to materials from group 1.1 according to the ISO/TR 15608 standard). In addition, the aforesaid hardness distributions were smooth and arranged symmetrically.

The macroscopic observations were performed in accordance with the guidelines specified in the PN-EN ISO 17639 standard. Imperfections were assessed on the basis of the

guidelines specified in the PN-EN ISO 5817 standard. The observations also involved the use of the catalogue of imperfections according to the PN-EN ISO 6520-1 standard. The macroscopic observations revealed the presence of welding imperfections referred to in the above-named standards. The imperfections were related to shape geometry (502, 503, 512 and 5214). All of the detected imperfections (except for 502, 503, 512 and 5214) did not exceed the limit values related to quality level B according to the PN-EN ISO 5817 standard. The previously enumerated imperfections were categorised as representing quality level C according to PN-EN ISO 5817.

The microscopic observations revealed the presence of the ferritic-pearlitic structure in the base material (cementite in pearlite, characterised by the lamellar and irregular structure). The fusion line of the butt joints contained the ferritic structure with traces of pearlite (specimens BW2 and BW4 revealed the presence of ferrite having the bainitic structure in the weld material). Specimen BW4 revealed welding imperfections in the form of microporosity. The fusion line of the T-joint contained the martensitic-bainitic structure and irregularly arranged banded grains of ferrite. Welding imperfections were not revealed.

In all of the specimens the weld area of the butt joints contained the ferritic structure. Specimen BW1 contained Widmannstätten structure. All of the specimens contained welding imperfections in the form of microporosity. The welds of the T-joints revealed the structure containing granular and acicular ferrite with areas of quasi-eutectoid. All of the specimens contained discontinuities in the form of microporosity.

The HAZ area of the butt joints contained grains of ferrite (all specimens). Widmannstätten structure was revealed in specimen BW1 and BW4. The grain boundaries in specimen BW3 copper (alloying element). Specimens BW1 and BW3 contained welding imperfections in the form of microporosity. The HAZ of the T-joint

contained the ferritic structure (specimens FW2-FW3: acicular ferrite) with martensitic areas. Specimens FW1 and FW3 contained welding imperfections in the form of microporosity.

References

- [1] Kasińska M., Towarnicki K., Piwowarczyk T., Ambroziak A.: *Badania złączy spawanych ze stali P265GH wykonanych z zastosowaniem różnych mieszanek gazowych oraz gatunków drutów spawalniczych*. Przegląd Spawalnictwa, 2016, vol. 88.
<http://dx.doi.org/10.26628/ps.v88i8.643>
- [2] <http://www.pse.pl>
- [3] <http://www.rynek-energii-elektrycznej.cire.pl>
- [4] Dobrzański J.: *Materiałoznawcza interpretacja trwałości stali dla energetyki*. Open Access Library, 2011, vol. 3, pp. 1-228.
- [5] Adamiec J., Januszkiewicz M.: *Ocena odporności na korozję wysokotemperaturową złączy spawanych laserowo rur ożebrowanych wykonanych ze stopów niklu*. Przegląd Spawalnictwa, 2015, vol. 87, no. 10.
<http://dx.doi.org/10.26628/ps.v87i10.495>
- [6] Dobosiewicz J., Zbroińska-Szczechura E.: *Ocena stopnia zużycia ciśnieniowych elementów kotłów pracujących w warunkach pełzania*. Energetyka, 2007, no. 12, pp. 917-922.
- [7] Trzeszczyński J.: *Monitorowanie pracy urządzeń cieplno-mechanicznych jako istotny element prognozowania ich żywotności w ostatniej fazie wydłużonej eksploatacji*. Energetyka, 2009, no. 12, pp. 129-131.
- [8] Jasiński A.: *EIP-online.pl*, 2014, no. 1(2), pp. 8-12.
- [9] Dobosiewicz J., Zbroińska-Szczechura E.: *Wytyczne oceny spoin, kolan rurociągów i komór pracujących w warunkach pełzania*. Energetyka, 2009, no. 12, pp. 123-128.
- [10] Dobrzański J., Paszkowska H., Kowalski B., Wodzyński J.: *Diagnostyka urządzeń energetycznych pod działaniem ciśnienia w podwyższonej temperaturze*. Prace IMŻ, 2010, no. 1, pp. 33-41.
- [11] Dobrzański J.: *Diagnostyka uszkodzeń elementów ciśnieniowych urządzeń energetycznych w ocenie przyczyn powstawania awarii na podstawie badań materiałowych*. Prace IMŻ, 2009, no. 2, pp. 36-45.
- [12] Zieliński A., Dobrzański J.: *Ocena stanu i przydatności do dalszej pracy materiału rurociągów parowych eksploatowanych powyżej obliczeniowego czasu pracy*. Prace IMŻ, 2013, no. 3, pp. 42-54.
- [13] Dobrzański J., Cieśla M.: *Wpływ długotrwałej eksploatacji na zmianę właściwości użytkowych materiału komór przegrzewacza pary pracujących w warunkach pełzania wykonanych z martenzytycznej stali X20CrMoV11-1*. Prace IMŻ no. 4, pp. 23-38, 2013.
- [14] Dobrzański J., Zieliński A., Paszkowska H.: *Wyznaczanie trwałości resztkowej i czasu dalszej bezpiecznej eksploatacji na przykładzie materiału rodzimego złącza spawanego*. Prace IMŻ, 2009, no. 1, pp. 9-25.
- [15] Wytyczne Urzędu Dozoru Technicznego no. 1/2015: *Zasady diagnostyki i oceny trwałości eksploatacyjnej elementów kotłów i rurociągów pracujących w warunkach pełzania*, UDT, edycja 27.10.2015
- [16] Józwick T.: *Wytyczne UDT no. 1/2015 – dokument mający znaczący wpływ na wzrost bezpieczeństwa eksploatacyjnego w sektorze wytwarzania energii elektrycznej*. Spajanie Materiałów Konstrukcyjnych, 2016, no. 3 (33).